Analysis of the X-ray emission of OB stars II: B stars

Elizaveta Ryspaeva[1,2] and Alexander Kholtygin[2,3]

[1] Crimean Astrophysical Observatory, Nauchny, Crimea, Russia; *e.ryspaeva@yandex.ru*
[2] Saint-Petersburg State University, Saint-Petersburg, Russia; *afkholtygin@gmail.com*
[3] Institute of Astronomy, Russian Academy of Sciences, Russia

Abstract This paper is the second part of an investigation into the mechanism for the origin of X-rays in early-type stars. Archival X-ray observations of 25 B stars, obtained by the *XMM-Newton* satellite, are analysed. We check two hypotheses on the origin of X-ray emission: the Magnetically Confined Wind Shock Model (MCWS) and Pollock's paradigm. For all studied stars, the mean ratio of the half widths at half maximum to the terminal velocities appears to be $R \approx 0.15 - 0.20$ in contradiction to Pollock's hypothesis that $R \approx 0.5$. We checked three possible consequences of the MCWS model: correlations between the hardness of the X-ray spectra for B stars and terminal wind velocities, mass loss rates and magnetic fields. It was shown that such correlations are marginal or even absent both for magnetic and non-magnetic B stars.

Key words: stars: early-type — stars: spectra: X-ray

1 INTRODUCTION

The X-ray emission from early-type OB stars can be formed as a result of instability in the stellar wind (see e.g., Feldmeier et al. 1997, Oskinova et al. 2006; Oskinova 2016; Oskinova et al. 2017). The generation of X-ray spectra by magnetic OB stars can be mainly described in the framework of the Magnetically Confined Wind Shock model (MCWS, Babel & Montmerle 1997).

In the paper by Ryspaeva & Kholtygin (2018) (hereafter Paper I), possible consequences of the MCWS model for 32 magnetic and non-magnetic O stars were investigated. In this paper, we assume that hardness of the X-ray spectrum should grow with increasing stellar parameters, such as terminal wind velocity, mass loss rate and stellar magnetic field. However, no such dependences for O stars were detected. This means that the above-mentioned consequences of the MCWS model are neither valid for magnetic O stars, nor for non-magnetic O stars. In addition, Ryspaeva & Kholtygin (2017, 2018) found that Pollock's paradigm formulated firstly by Pollock (2007) for O star ζ Ori is incorrect.

Many B type stars with effective temperature of about 10 000–18 000 K are strong X-ray sources. The effective temperatures of B stars are lower than those of O stars. Therefore, it may be suggested that the mechanism of X-ray emission formation for B stars can differ from that for O stars. In the present paper, we investigate whether con-

sequences of the MCWS model checked in Paper I are valid for B stars. We also try to ascertain whether or not Pollock's paradigm is correct for B stars.

In Section 2 the parameters of considered stars and the data reduction procedure are described. A new approach for the method of spectral line identification is given in Section 3. The results of checking Pollock's hypothesis for B stars are presented in Section 4. The possible consequences of the MCWS model for B stars are considered in Section 5. Discussion of the results and final conclusions are provided in Section 6.

2 OBSERVATION AND DATA REDUCTION

We have analysed the archival X-ray observations of 25 B stars obtained by the *XMM-Newton* satellite in 2000–2015. The parameters of these stars and corresponding references are reported in Table 1. From the list of stars given in the table, we see that eight objects are variable, and four stars have very strong lines in their spectra relative to the continuum level.

The log of observations is written in Table 2. The data reduction was made by SAS 14.0 software following the recommendation given by the SAS team[1]. Firstly, we extracted and merged spectra from the first order of RGS1 and RGS2 spectrometers using *rgsproc* script. Thereafter,
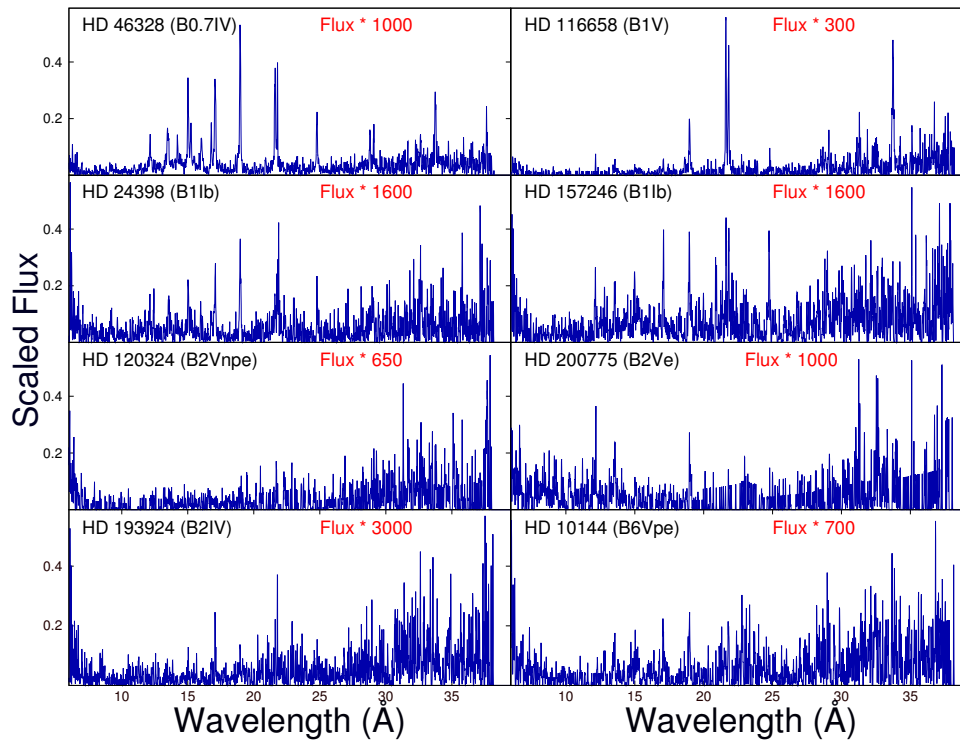
---

[1] *www.cosmos.esa.int/web/xmm-newton*

Fig. 1 Scaled X-ray spectra of selected B stars.

we filtered observations from background flares using the *tabgtigen* and *rgsfilter* tasks. If a studied object was observed several times, we combined the spectra from different sets using the *rgscombine* task.

For seven objects from the list of these B stars (HD 24398, HD 46328, HD 10144, HD 116658, HD 120324, HD 157246 and HD 193924) the spectra obtained by *XMM-Newton* were not yet published. X-ray spectra of these stars extracted by us together with spectra of Herbig Be star HD 200775 for comparison are displayed in Figure 1. These spectra are scaled for better visibility. In the final spectra we consider the wavelength interval from 6 to 40 Å. The AtomDB database[2] was used for line identification.

3 SPECTRAL ANALYSIS AND LINE IDENTIFICATION

To check the examined hypotheses about the formation of X-ray spectra, we must identify lines in the X-ray spectra and determine their parameters. These parameters are: full width at half maximum (FWHM), ratio of half width at half maximum (HWHM) to the wind terminal velocity $HWHM/v_\infty$, maximum flux for the line and spectral hardness. The last value is the ratio of the maximum fluxes for the lines belonging to ions of adjacent ionization stages.

For spectral line identification, we use the method described in Section 3 of Paper I. The blends were approximated by the sum of Gaussians or Gaussian-like functions using equations (2)−(4) in Paper I. Figure 2 demonstrates how the blends can be resolved. For all approximative lines, we calculated FWHM by equation (6) and equation (7) in Paper I. For weak isolated lines contributing only 7−10 data points inside the line profile, the FWHM values were calculated by numerical integration using equation (8) in Paper I. We employed the following procedure. First, we resolved all possible blends using the AtomDB database. Second, we select those cases which produce a set of lines with close wavelengths for at least 10 stars. The sample of lines resolved in such a way is given in Table 3. These lines are applied to estimate the spectral hardness, as a ratio of the maximum fluxes of ions in adjacent stages of ionization. For example, we calculated hardness as a ratio of maximum intensities for ions Fe XX/Fe XIX, Ca XIII/Ca XII and Ar XIII/Ar XII given in Table 3.

We analyse the statistics associated with all possible types of detected lines; 72.9% of such lines are identified by fitting the observed profiles, 27.1% of possible lines are considered as single and their FWHMs are estimated by a numerical method; for 18.1% the local continuum can be extracted from the spectra and 1.5% of lines appear to be blue- or redshifted. One can see examples of shifted lines in Figure 2. This statistical result lets us conclude

² *www.atomdb.org*

Table 1 The List of Targets

HD (1)	Spectral type (2)	v_∞ (km s^{-1}) (3)	Ref (4)	$\log(\dot{M})$ ($M_\odot$yr^{-1}) (5)	Ref (6)	B_p (G) (7)	Ref (8)	Notes (9)
3360	B2IV	942	[2]	−8.4	[2]	340	[6]	PVS
10144	B3 Ve	1330	[3]	−10.4	[3]	-	-	Be star
21856	B1V	500	[4]	−8.2	[4]	-	-	
24398	Bl Ib	1295	[1]	-	-	-	-	Vary
37128	B0 la	1910	[1]	−5.6	[6]	-	-	BS
46328	B1 III	1984	[5]	-	-	1500	[6]	β Cep
63425	B0.5V	2478	[2]	−7.9	[2]	460	[6]	
64760	B0.5 Ib	1500	[1]	-	-	-	-	
66665	B0.5V	2008	[2]	−8.2	[2]	670	[6]	
116658	B1IV	1750	[3]	−8.0	[3]	-	-	β Cep
120324	B2 IV–Ve	1470	[3]	−9.1	[3]	-	-	Be Star
122451	B1III	1552	[2]	−8.0	[2]	250	[6]	β Cep
127381	B1-2V	2186	[2]	−9.7	[2]	500	[6]	EVS
136504	B2IV–V	1019	[2]	−8.3	[2]	600	[6]	Binary
143275	B0.2IVe	1100	[4]	−6.9	[4]		-	
149438	B0.2V	2176	[2]	−7.6	[2]	200	[6]	
152234	B0.5Ia	1450	[1]	-	-	-	-	
157246	B1 Ib	735	[1]	-	-	-	-	
158926	B1.5 IV	1560	[3]	−8.4	[3]	-	-	β Cep
165024	B2 Ib	1185	[1]	-	-	-	-	
175191	B3 IV	1220	[3]	−9.9	[3]	-	-	HPM
182180	B2Vn	1058	[2]	−9.9	[2]	11000	[6]	
193924	B2.5V	1360	[3]	−9.9	[3]	-	-	Binary
200775	B2Ve	862	[2]	−8.1	[2]	1000	[6]	HAEBE
205021	B1IV	2169	[2]	−8.6	[2]	360	[6]	β Cep

HD number is given in the first column. Spectral type (second column) and terminal velocities (third column) are taken from the sources written in col. (4). Mass loss rates and corresponding references are presented in cols. (5) and (6) respectively. Polar magnetic field B_p and corresponding references are reported in cols. (7) and (8) respectively. Comments (taken from the SIMBAD database) are in the last column.

References: [1] Howarth et al. (1997); [2] Nazé et al. (2014); [3] Cohen et al. (1997); [4] De Becker et al. (2017); [5] Kurapati et al. (2017); [6] Petit et al. (2013).

Notes: PVS – Pulsating variable star; Vary – Variable star; BS - Blue supergiant; β Cep – Variable Star of β Cep type; EVS – Ellipsoidal variable star; HPM – High proper-motion; HAEBE – Ae/Be Herbig star.

that X-ray spectral lines are formed in stellar winds with clumps. A large part of clumps has a slab-like form, but there are spherical clumps in stellar winds (see Oskinova et al. (2006) for details), and 0.1% of lines in the analyzed spectra of B stars appear to be redshifted.

4 CHECKING POLLOCK'S PARADIGM

The distributions of number of lines in different intervals of the ratio HWHM/v_∞ are analysed. These distributions for magnetic (left panel) and nonmagnetic (right panel) B-stars are presented in Figure 3. Inasmuch as the observed line profiles can be fitted with different numbers of contributed lines, we chose the most accurate approximations of the same profile with the smallest number of lines and with the biggest number of contributed lines. Thus we fix the smallest and largest number of possible lines that can be identified in the spectra. Left bars in both panels of Figure

3 indicate the biggest numbers of possible lines in stellar spectra, while right bars indicate the smallest.

After inspecting Figure 3, we can conclude that most lines in the spectra of the examined B stars have the ratio HWHM/v_∞ in the interval $5-15\%$. The same result was established for O stars by Ryspaeva & Kholtygin (2017) and in Paper I. It means that Pollock's paradigm is hardly also valid for B stars. So, we conclude that this paradigm is neither correct for O stars nor for B stars.

In addition, when considering Figure 3, we see that the ratio HWHM/v_∞ decreases for magnetic stars significantly faster than for non-magnetic stars. This fact probably indicates that the region of X-ray formation for magnetic stars is much more compact than that for non-magnetic ones. It means that our statistical result for non-magnetic B stars gives a more reliable contradiction to Pollock's paradigm.

The failure of Pollock's paradigm may be explained by rapid cooling of hot gas behind the shock in the zone $v \approx v_\infty$. This means that gas in this zone does not emit

Table 2 Log of Observations

Object (1)	ObsID (2)	Obs.date (3)	Exp. (s) (4)	Object (5)	ObsID (6)	Obs.date (7)	Exp. (s) (8)
HD 3360	0600530301	3.08.2009	13 000	HD 165024	0302020201	12.10.2005	72 700
HD 10144	042120101	7.12.2006	13 680	HD 175191	0721210101	22.09.2013	8000
HD 21856	0743660301	3.03.2015	33 000	HD 182180	0690210401	25.09.2012	12 000
HD 24398	0201550201	13.02.2004	41 100	HD 193924	0690680201	20.03.2013	71 000
HD 37128	0112400101	6.03.2002	13 153	HD 200775	0650320101	30.08.2010	11 916
HD 46328	0691900101	16.10.2012	10 2000	HD 149438	0112540101	20.08.2001	19 001
HD 63425	0671990201	6.05.2011	21 200		0112540201	20.08.2001	7300
HD 64760	0401050201	16.03.2007	68 788	HD 152234	0109490101	5.09.2001	33 870
HD 66665	0671990101	29.10.2011	37 700		0109490201	6.09.2001	33 773
HD 116658	0690680101	6.07.2012	13 000		0109490301	7.09.2001	35 009
HD 120324	0402121701	15.02.2007	11 150		0109490401	8.09.2001	31 873
HD 122451	0150020101	19.07.2003	57 623		0109490501	9.09.2001	31 664
HD 127381	0690210101	10.08.2012	8000		0109490601	10.09.2001	33 505
HD 136504	0690210201	4.03.2013	9000	HD 205021	0300490201	27.07.2005	41 100
HD 143275	0743660101	7.03.2015	31 200		0300490301	29.07.2005	39 300
HD 157246	0201550101	22.02.2004	27 600		0300490401	2.08.2005	43 200
HD 158926	0690200101	4.03.2013	31 200		0300490501	6.08.2005	41 100

The object names are listed in cols. (1) and (5). In cols. (2) and (6) we provide the observation ID numbers. Date of the observation and exposure time in seconds are presented in cols. (3) and (4), and (7) and (8) respectively.
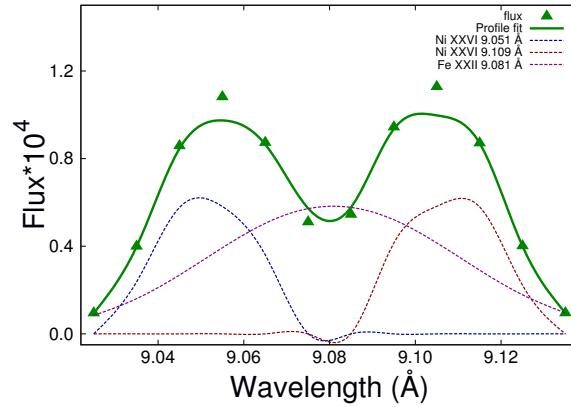

Fig. 2 An example of observed line profile approximation in the spectrum of star HD 175191. The line corresponding to Ni XXVI 9.109 Å is redshifted.
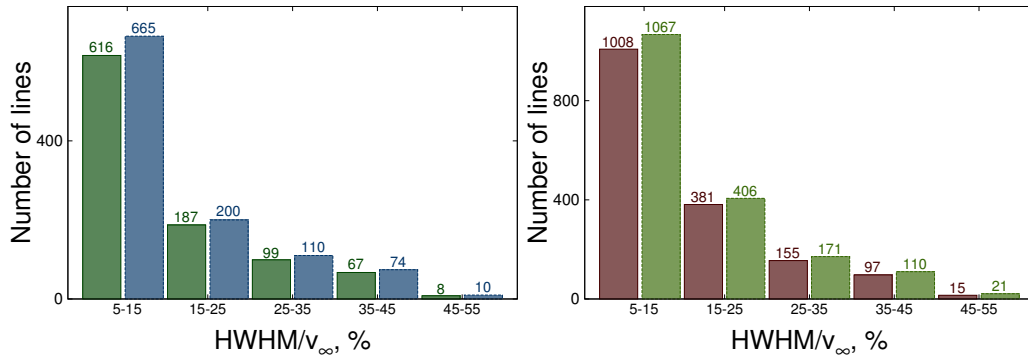

Fig. 3 The distribution of the HWHM/v_∞ ratio for magnetic (*left panel*) and non-magnetic (*right panel*) B stars. The left bars in each plot demonstrate the minimum possible number of spectral lines in the considered intervals of these ratios; right bars show the maximum number of such lines (see text).

Table 3 Examples of Sets of Lines with Close Wavelengths in Spectra of at Least 10 Stars

Wavelength (Å) (1)	Flux (10^{-5}) (2)	FWHM (km s^{-1}) (3)	Object (4)	Wavelength (Å) (5)	Flux (10^{-5}) (6)	FWHM (km s^{-1}) (7)	Object (8)
Ca XIV				Ca XIII			
24.265	8.490	181	HD 120324	26.055	9.086	138	HD 116658
24.155	4.998	207	HD 143275	25.965	9.274	294	HD 136504
24.080	11.246	114	HD 149438	26.095	5.119	122	HD 143275
24.105	5.315	403	HD 152234	26.39	12.959	517	HD 149438
24.155	2.601	337	HD 157246	26.12	1.498	236	HD 152234
24.185	4.076	835	HD 158926	26.015	4.899	134	HD 157246
24.155	2.813	193	HD 165024	25.965	4.385	169	HD 158926
24.025	5.990	238	HD 175191	26.115	2.750	164	HD 165024
24.005	2.780	363	HD 193924	26.065	1.976	110	HD 182180
24.085	3.820	233	HD 205021	25.955	2.064	244	HD 193924
24.145	2.861	139	HD 21856	26.105	5.373	282	HD 205021
24.076	15.303	385	HD 37128	26.015	5.131	101	HD 21856
24.105	2.185	536	HD 46328	26.057	9.956	300	HD 37128
24.015	8.336	236	HD 63425	26.015	4.049	369	HD 46328
24.255	2.737	437	HD 64760	26.135	8.053	152	HD 63425
24.035	1.596	356	HD 66665	26.065	7.261	225	HD 64760
24.145	4.284	111	HD 116658	26.035	4.280	100	HD 66665
				26.135	8.993	115	HD 10144
Ar XII				Ar XI			
31.415	15.433	191	HD 120324	34.335	51.035	168	HD 136504
31.415	9.924	255	HD 122451	34.085	6.402	120	HD 143275
31.365	18.771	234	HD 127381	34.330	24.895	276	HD 149438
31.355	13.168	217	HD 143275	34.345	6.477	147	HD 157246
31.355	23.590	304	HD 149438	34.365	11.532	386	HD 158926
31.365	1.983	281	HD 152234	34.625	2.890	124	HD 165024
31.565	7.855	293	HD 157246	34.615	37.594	110	HD 175191
31.305	44.842	110	HD 158926	34.261	30.103	124	HD 182180
31.595	11.911	117	HD 165024	34.025	3.581	153	HD 193924
31.295	72.762	141	HD 175191	34.035	11.175	231	HD 205021
31.385	11.502	273	HD 193924	34.347	6.629	133	HD 21856
31.555	10.062	127	HD 200775	34.615	9.438	149	HD 24398
31.345	10.814	217	HD 21856	34.095	20.285	114	HD 3360
31.305	5.527	155	HD 24398	34.436	21.857	326	HD 63425
31.395	14.771	139	HD 3360	34.385	6.823	200	HD 66665
31.385	16.548	123	HD 63425	34.325	16.789	152	HD 122451
31.599	5.622	384	HD 64760				
31.325	6.436	217	HD 66665				
31.385	44.289	147	HD 116658				
Fe XX				Fe XIX			
12.836	0.102	335	HD 116658	15.308	2.406	1397	HD 116658
12.805	8.678	989	HD 122451	15.169	11.227	1054	HD 122451
12.610	2.253	185	HD 143275	15.227	0.832	520	HD 127381
12.585	8.097	736	HD 158926	15.214	48.284	1436	HD 149438
12.835	5.629	105	HD 182180	15.035	2.433	351	HD 165024
12.585	5.175	134	HD 200775	15.206	6.496	132	HD 182180
12.805	4.158	1000	HD 24398	15.046	2.081	199	HD 193924
12.816	2.188	404	HD 63425	15.306	3.992	467	HD 200775
12.837	1.194	1329	HD 64760	15.043	9.113	1098	HD 205021
12.798	3.262	731	HD 66665	15.156	0.647	446	HD 175191
12.710	8.315	1210	HD 37128				

Sets of lines with close wavelengths (listed in cols. (1) and (5)) used for the spectral hardness calculations. Cols. (2) and (6) give the maximum flux counts (in photons per second) in the line profiles. In cols. (3) and (7), the FWHMs values are presented. HD numbers are listed in cols. (4) and (8).
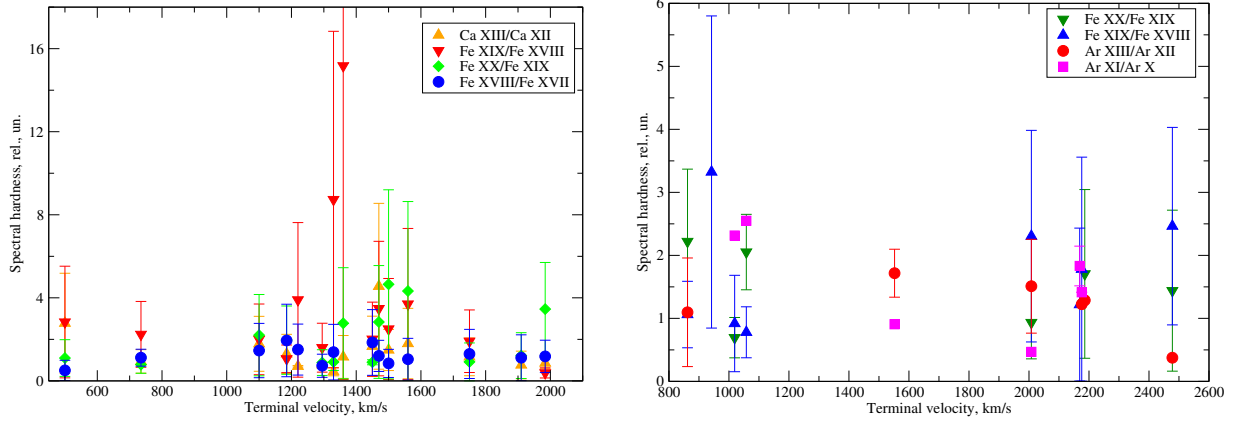
Fig. 4 *Left:* the spectral hardness vs. terminal velocities for non-magnetic B stars. *Right:* the same as in the left panel but for magnetic B stars.
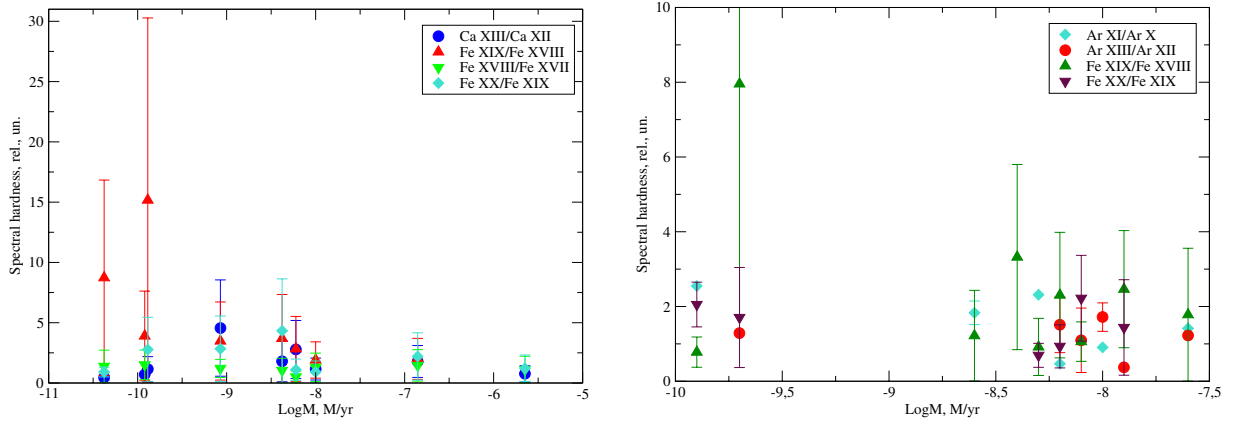

Fig. 5 *Left:* the spectral hardness vs. mass loss rate for non-magnetic B stars. *Right:* the same as in the left panel but for magnetic B stars.
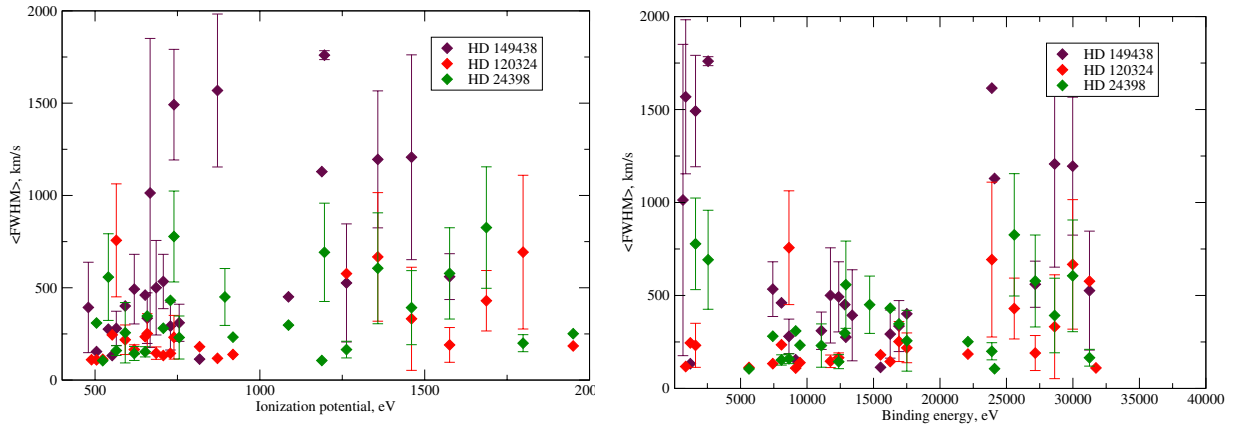

Fig. 6 The dependence of average FWHM on the ionisation potential (*left panel*) and on binding energy (*right panel*) for spectral lines from each ion for three stars.

in X-ray. This also implies that the bulk of X-ray lines is formed close to the stellar surface where the gas velocity $v \ll v_\infty$ both for O and for B stars.

5 CHECKING THE CONSEQUENCES OF THE MCWS MODEL

We considered the three above mentioned possible consequences of the MCWS model for B stars. The spectral hardness is calculated using the most reliable line identi-
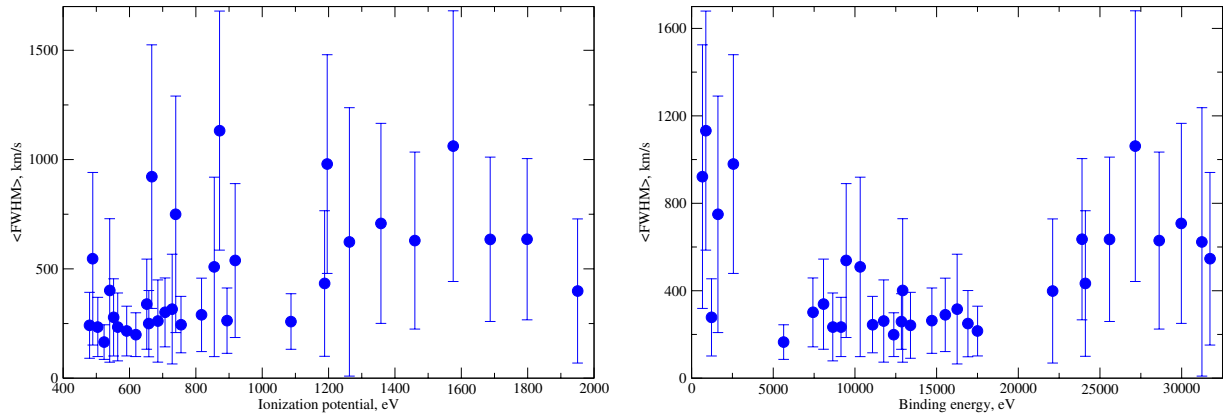
Fig. 7 The dependence of average FWHM on the ionisation potential (*left panel*) and on binding energy (*right panel*) for spectral lines from each ion in spectra of all studied stars.

fications (see Sect. 2). We calculate the spectral hardness as a ratio of the observed fluxes for the lines listed in the left part of Table 3 to those given in the right part for ions Ca XIII/XII, Ar XII/XI, Fe XX/XIX and others.

The correlations between the spectral hardness and terminal velocity, mass loss rate and magnetic field are analysed. In Figure 4 (left panel) the plot of spectral hardness vs. terminal wind velocity for non-magnetic B stars is presented. Figure 4 (right panel) shows this correlation for magnetic B stars.

The dependence of the spectral hardness on mass loss rate is displayed in Figure 5 (left panel) for non-magnetic stars and in Figure 5 (right panel) for magnetic stars. ud-Doula et al. (2014) predicted the trend that lower mass-loss rate leads to lower hardness. Our study does not confirm this conclusion. Note that the direct connection proposed by ud-Doula et al. (2014) between the cooling efficiency $\log \varepsilon_c$ and mass-loss rate $\dot{M}$ can fail if (as we propose) the X-ray emission is formed close to the stellar surface. Moreover, determination of the spectral hardness introduced by them differs from that used by us.

In addition, we have estimated the average value of FWHM for all suitable lines in the spectra of the considered B stars. Then we calculated the average FWHM of all lines from each ion in one stellar spectrum. The dependences between these average FWHM and their ionization potentials and binding energy (in eV) were analysed. Figure 6 depicts such correlations for a sample of three stars. We also calculate the average FWHM of lines from the same ion in many stellar spectra. These correlations for all studied stars are demonstrated in Figure 7. Values of ionization potentials and binding energies were taken from the ASD database[3].

---

[3] *https://physics.nist.gov/PhysRefData/ASD/ionEnergy.html*

6 DISCUSSION AND CONCLUSIONS

6.1 X-ray Variability

Some stars in our sample are variable or belong to the β Cep type. However, all such stars were observed in the X-ray range with long exposures but were not observed multiple times. The bulk of the X-ray data for these stars does not show line profile variability. Therefore, we will neglect possible variations in the X-ray line profile. We can consider all observed line profiles to be stable.

6.2 Pollock's Paradigm

The results of our work demonstrate that Pollock's paradigm is not correct for B stars. Inasmuch as B type stars have lower effective temperatures than O stars, Pollock's paradigm can be suitable for B-stars. Therefore in our present paper we have checked this hypothesis for such objects. Our results demonstrate that Pollock's paradigm is not correct for B stars. This fact together with results of the papers by Ryspaeva & Kholtygin (2017) and Paper I lets us conclude that, both in O and B stars, most X-ray emission is produced mainly in dense regions very close the star.

6.3 The MCWS Model

As we can see from analysing Figures 4–5, there is no correlation between the X-ray spectral hardness and terminal wind velocity, and the same is true for mass loss rate both for magnetic and non-magnetic B stars. A similar result for O type stars was demonstrated in Paper I. The absence of such a correlation can only be explained if most of the X-rays formed near the star's surface, in accordance with our previous conclusion.

The same proposal was made by us from the analysis of X-ray spectra of O stars (see Paper I). In the case of B

stars, the region of formation for X-ray radiation is probably even narrower than that for O stars due to the lower mass loss rate for early B stars. This radiation stratification for B stars is practically absent, which explains the lack of correlation between ionization potential and binding energy of atoms and ions, and FWHMs of X-ray lines.

6.4 Redshifted Lines

Most lines in the spectra of stars studied by us have symmetric profiles. Such profile shapes can be interpreted in the framework of the model by Oskinova et al. (2006, their sect. 8.4) assuming that most of the clumps in the winds of B stars have a flat ("pancake") shape.

At the same time, a small number of lines in our spectra are blue- or redshifted. Those lines that are blueshifted can be interpreted using the model by Oskinova et al. (2006) and assuming that some of the clumps in the wind are spherical with isotropic opacity. At the same time, 0.1% of lines in the spectra under study (see Sect. 3) are redshifted.

Such a displacement cannot be explained in the model by Oskinova et al. (2006). However, it can be assumed that since our results show that the X-ray radiation is formed near the star's photosphere, the region of X-ray formation can be considered as the pseudo-photosphere. In this case, the line shape can be interpreted within the framework of the classical Sobolev theory (see, for example, Sobolev (1960)). In the case of X-ray absorption by spherical clumps, the X-ray lines will be redshifted. Due to the small fraction of spherical clumps in the wind, the number of redshifted lines will be small as it is in our case.

7 GENERAL CONCLUSIONS

Thus, after carrying out a comparative description and analysis, it became possible to arrive at the following conclusions:

– The most probable value of the ratio of HWHM for lines in the spectra of all considered B stars to the wind terminal velocity belongs in the interval $5-15\%$. This contradicts the Pollock (2007) paradigm of X-rays formulated for O stars. Therefore, one can conclude that the X-ray emissions of B stars originate mainly in regions close to the stellar surface as well as X-ray emission for O stars.

– We analysed possible consequences of the MCWS model for X-rays both for magnetic and non-magnetic B stars. It was revealed that the consequences from the MCWS model that we considered are not confirmed. It is worth noting that the absence of the dependence

of X-ray spectral hardness on stellar parameters can be easily explained if the X-ray emission (as we claim) is formed close to the star.

– Analysing the shape of the X-ray line profiles for all considered B stars, one can conclude that the main bulk of these lines has a symmetrical Gaussian or Gaussian-like shape. This could mean that inhomogeneous stellar winds from B stars contain mainly slab-like clumps.

– In contrast to the case of O stars, we did not find any dependence between the FWHM for X-ray lines and an ion's ionization potential and its binding energy. This could mean that there is no ion stratification in the wind of B stars. Again this can be explained if all spectral lines are formed in the narrow zone near the stellar surface.

References

Babel, J., & Montmerle, T. 1997, A&A, 323, 121

Cohen, D. H., Cassinelli, J. P., & MacFarlane, J. J. 1997, ApJ, 487, 867

De Becker, M., del Valle, M. V., Romero, G. E., Peri, C. S., & Benaglia, P. 2017, MNRAS, 471, 4452

Feldmeier, A., Kudritzki, R.-P., Palsa, R., Pauldrach, A. W. A., & Puls, J. 1997, A&A, 320, 899

Howarth, I. D., Siebert, K. W., Hussain, G. A. J., & Prinja, R. K. 1997, MNRAS, 284, 265

Kurapati, S., Chandra, P., Wade, G., et al. 2017, MNRAS, 465, 2160

Nazé, Y., Petit, V., Rinbrand, M., et al. 2014, ApJS, 215, 10

Oskinova, L. M. 2016, Advances in Space Research, 58, 739

Oskinova, L. M., Feldmeier, A., & Hamann, W.-R. 2006, MNRAS, 372, 313

Oskinova, L. M., Ignace, R., & Huenemoerder, D. P. 2017, in IAU Symposium, 329, The Lives and Death-Throes of Massive Stars, eds. J. J. Eldridge, J. C. Bray, L. A. S. McClelland, & L. Xiao, 151

Petit, V., Owocki, S. P., Wade, G. A., et al. 2013, MNRAS, 429, 398

Pollock, A. M. T. 2007, A&A, 463, 1111

Ryspaeva, E. B., & Kholtygin, A. F. 2017, Astronomische Nachrichten, 338, 959

Ryspaeva, E., & Kholtygin, A. 2018, RAA (Research in Astronomy and Astrophysics), 18, 104 (Paper I)

Sobolev, V. V. 1960, Moving Envelopes of Stars (Cambridge: Harvard Univ. Press, 1960)

ud-Doula, A., Owocki, S., Townsend, R., Petit, V., & Cohen, D. 2014, MNRAS, 441, 3600